Article

Cell

Anti-HA Glycoforms Drive B Cell Affinity Selection and Determine Influenza Vaccine Efficacy

Graphical Abstract

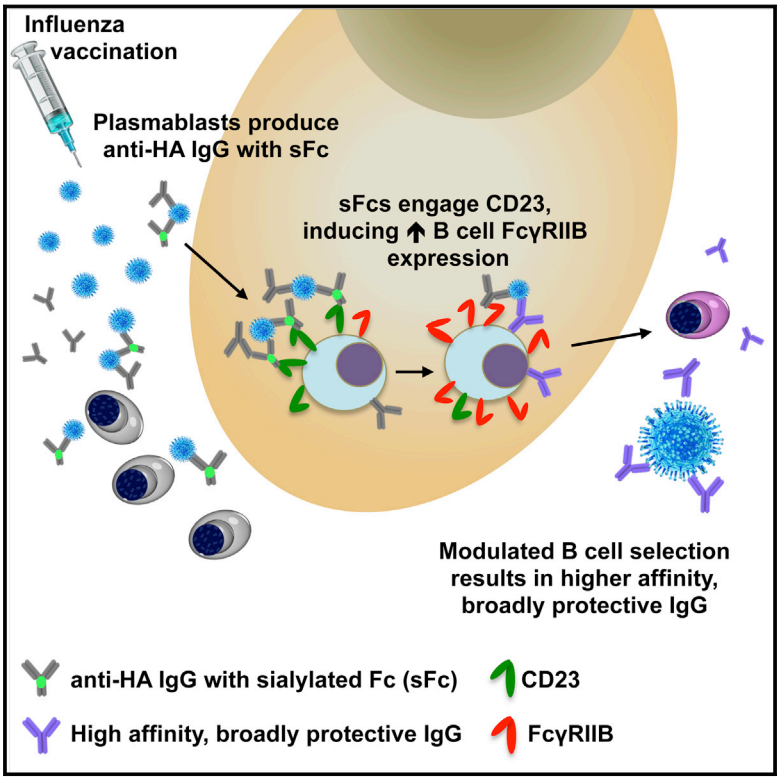

Authors

Taia T. Wang, Jad Maamary, Gene S. Tan, ..., Peter Palese, Rafi Ahmed, Jeffrey V. Ravetch

Correspondence

ravetch@rockefeller.edu

In Brief

The glycan composition of the Fc region of anti-influenza antibodies changes following vaccination, with sialylated Fc glycan abundance predicting the quality of the vaccine response and production of high-affinity antibodies against the conserved stalk domain of the influenza HA.

Highlights

- Dynamic changes in Fc glycan composition following influenza vaccination
- Sialylated Fc glycan abundance on anti-HA IgG predicts vaccine response
- Sialylated Fc immune complexes engage CD23 and BCR to modulate affinity maturation
- IgGs elicited by sialylated Fc immune complexes protect broadly against H1 viruses

Wang et al., 2015, Cell *162*, 160–169
July 2, 2015
http://dx.doi.org/10.1016/j.cell.2015.06.026

CellPress

Cell

Article

Anti-HA Glycoforms Drive B Cell Affinity Selection and Determine Influenza Vaccine Efficacy

Taia T. Wang,[1,7] Jad Maamary,[1,7] Gene S. Tan,[2] Stylianos Bournazos,[1] Carl W. Davis,[4,5] Florian Krammer,[2] Sarah J. Schlesinger,[6] Peter Palese,[2,3] Rafi Ahmed,[4,5] and Jeffrey V. Ravetch[1,*]

[1]The Laboratory of Molecular Genetics and Immunology, The Rockefeller University, 1230 York Avenue, New York, NY 10065, USA
[2]Department of Microbiology, Icahn School of Medicine at Mount Sinai, New York, NY 10029, USA
[3]Division of Infectious Diseases, Department of Medicine, Icahn School of Medicine at Mount Sinai, New York, NY 10029, USA
[4]Department of Microbiology and Immunology, Emory University School of Medicine, Atlanta, GA 30322, USA
[5]Emory Vaccine Center, Emory University School of Medicine, Atlanta, GA 30322, USA
[6]Laboratory of Molecular Immunology, The Rockefeller University, New York, NY 10065, USA
[7]Co-first author
*Correspondence: ravetch@rockefeller.edu
http://dx.doi.org/10.1016/j.cell.2015.06.026

SUMMARY

Protective vaccines elicit high-affinity, neutralizing antibodies by selection of somatically hypermutated B cell antigen receptors (BCR) on immune complexes (ICs). This implicates Fc-Fc receptor (FcR) interactions in affinity maturation, which, in turn, are determined by IgG subclass and Fc glycan composition within ICs. Trivalent influenza virus vaccination elicited regulation of anti-hemagglutinin (HA) IgG subclass and Fc glycans, with abundance of sialylated Fc glycans (sFc) predicting quality of vaccine response. We show that sFcs drive BCR affinity selection by binding the Type-II FcR CD23, thus upregulating the inhibitory FcγRIIB on activated B cells. This elevates the threshold requirement for BCR signaling, resulting in B cell selection for higher affinity BCR. Immunization with sFc HA ICs elicited protective, high-affinity IgGs against the conserved stalk of the HA. These results reveal a novel, endogenous pathway for affinity maturation that can be exploited for eliciting high-affinity, broadly neutralizing antibodies through immunization with sialylated immune complexes.

INTRODUCTION

IC-FcR interactions mediate a wide array of cellular processes required for maturation of protective, vaccine-induced antibody responses, including efficient transport of antigen to the germinal center, activation of T follicular helper cells, and selection of high-affinity B cells. Indeed, FcR signaling is responsible, in large part, for maintaining the balanced positive and negative signaling that culminates in appropriate immune responses (Pincetic et al., 2014). Two basic classes of FcRs have been identified: type I FcRs are immunoglobulin superfamily members and include FcγRI, II, and III, while type II FcRs are C-type lectin family members and include DC-SIGN and CD23 (Figure 1A). Perturbations in either signaling arm result in changes in antibody affinity and peripheral tolerance (Bolland and Ravetch, 2000). IC-FcR interactions can initiate activating, inhibitory, or modulatory cell signaling depending on the pattern of FcRs engaged, which is determined by the structure of Fc domains within an IC. Fc structure, in turn, is regulated by IgG subclass and Fc glycan composition.

IgG antibodies exist as four subclasses in humans (IgG1-4) with IgG1 in highest abundance in serum followed by IgG2 > IgG3 > IgG4. This was demonstrated by the subclass distribution of baseline (pre-vaccination) anti-HA IgGs from this study's cohort of ten healthy adult volunteers (Figure 1B, Figure S1). Each subclass is distinct in its ratio of binding to activating:inhibitory type 1 FcγRs, with IgG1 and IgG3 having the highest activating receptor binding affinities (Figure 1C) (Bournazos et al., 2014; Morell et al., 1970).

The Fc glycan is an N-linked, complex, biantennary structure attached within the Cγ2 domain at Asn-297 of each IgG heavy chain and its presence is essential for all Fc-FcR binding interactions (Anthony and Ravetch, 2010). Composition of the core Fc glycan heptasaccharide can be modified by addition of specific saccharide units (fucose [F], N-acetylglucosamine [N], galactose [G] and sialic acid [S]) (Figure 1D); these modifications are dynamic and act to regulate the biological activity of IgG molecules by modulating Fc structure and, as a consequence, IC-FcR interactions. At baseline, a majority of IgG Fc glycoforms are of "neutral" composition, defined by the presence of fucose and absence of sialic acid (Figure 1E, neutral glycans represented by +N and −S, +F groups). sFc are present with an abundance of ~5%–20% (Figure 1E, +S group) and afucosylated glycoforms are found with an abundance of ~5%–15% (Figure 1E, −F group). This distribution was demonstrated by the baseline Fc glycoform composition on anti-HA IgG1 of this study's patient cohort (Figure 1E).

The most biologically significant modifications to Fc glycan composition are sialylation and fucosylation: the presence of sialic acid is inhibitory for type I Fc receptor binding, while the absence of fucose enhances binding to the activating type I FcγRIIIa. The presence of sialic acid alone is the determinant of Fc-type II FcR binding (Figure 1F) (Anthony et al., 2008b; Sondermann et al., 2013). Sialylation has the effect of increasing the conformational flexibility of the Cγ2 domain, enabling the Fc to

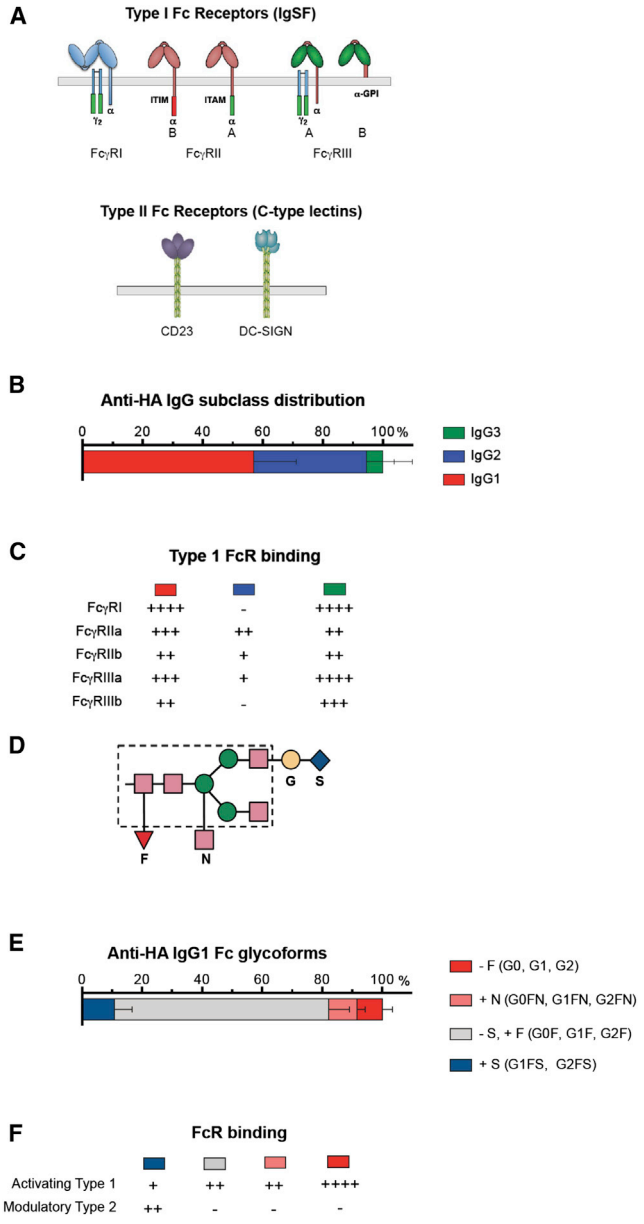

Figure 1. Type I and Type II FcR Binding Characteristics of Human Anti-HA IgG

(A) Overview of Type I and Type II FcR family.

(B) Subclass distribution of pre-vaccination anti-H1 HA (Cal/09) IgG from a cohort of ten healthy adults. Mean IgG1: 56.18% (SD 14.16), IgG2: 37.64% (SD 15.14), IgG3: 5.37% (SD 3.82). IgG4 levels were below the limit of detection.

(C) Type I FcR binding characteristics of IgG subclasses.

(D) Schematic overview of the Fc-associated glycan structure. Composition of the core Fc glycan (boxed) can be modified by addition of fucose (F), N-acetylglucosamine (N), galactose (G), and sialic acid (S) residues.

(E) Fc glycoform distribution on baseline anti-H1 HA IgG1 from our patient cohort.

(F) Effect of Fc glycoforms on binding to type I and type II FcRs. Fc glycovariants were categorized into: sialylated (blue; +S [G1FS, G2FS]), afucosylated (red; −F, [G0, G1, G2]) and "neutral," defined by the presence of fucose and absence of sialic acid (with branching GlcNAc in pink; +N, [G0FN, G1FN, G2FN], or without branching GlcNAc in gray; −S, +F [G0F, G1F, G2F]).

Error bars in (B) and (E) indicate SD. See also Figure S1.

sample a more "closed" conformation (Ahmed et al., 2014) thereby exposing binding sites for type II FcRs with correspondingly reduced type I FcR binding potential. Sialylation of the Fc glycan therefore represents a mechanism for regulating the effector activity of immunoglobulins through alternation of Fc conformations between open and closed states, thus regulating Fc binding to type I or type II FcRs, respectively (Sondermann et al., 2013). Studies on the bisecting GlcNAc modification show possible increased type I FcγRIIIa binding affinity; however, afucosylation is a far more potent determinant of strong FcγRIIIa binding (Hodoniczky et al., 2005; Shields et al., 2002; Shinkawa et al., 2003; Umaña et al., 1999). Addition of galactose alone to one or both arms of the branched Fc glycan does not affect FcR binding but is significant because galactosylation is a prerequisite for sialylation.

Shifting IgG Fc binding specificity from type I to type II FcRs can result in significant in vivo responses and precise regulation of sFc abundance is likely a fundamental homeostatic process. One known consequence of increasing type II FcR signaling is anti-inflammatory activity, a classic example of which is the therapeutic anti-inflammatory activity of high-dose intravenous immunoglobulin (IVIG) (Anthony et al., 2008a; Kaneko et al., 2006; Washburn et al., 2015). sFcs in IVIG, acting through binding of the type II FcR DC-SIGN on innate effector cells, stimulate IL-33 production resulting in downstream anti-inflammatory processes (Anthony et al., 2011). Disrupted balance in type I and type II FcR signaling likely occurs in several inflammatory diseases such as rheumatoid arthritis and granulomatosis with polyangiitis in which decreased abundance of sFc are found on autoantibodies such as anti-citrullinated peptide (ACPA) and anti-proteinase 3 (PR3) antibodies, respectively. Sialylation of anti-ACPA and anti-PR3 Fcs is reduced during disease flares, while disease remission is correlated with elevated Fc glycan sialylation of those autoantibodies (de Man et al., 2014; Espy et al., 2011; Scherer et al., 2010; Tomana et al., 1988; van de Geijn et al., 2009; Wuhrer et al., 2015).

Just as sialic acid-modified Fc glycans play a critical role in the regulation of inflammatory processes, the presence or absence of a branching fucose moiety modulates the interaction of IgG Fcs with FcγRIIIa to enhance or inhibit IgG-mediated ADCC and monocyte/macrophage activation (Umaña et al., 1999) (Shinkawa et al., 2003). Afucosylated Fc domains have increased affinity for the activating receptor FcγRIIIa that results from a stabilizing interaction between the N-glycan on FcγRIIIa with the afucosylated Fc glycan (Ferrara et al., 2011). Removal of fucose from monoclonal therapeutic antibodies such as rituximab and trastuzumab improved their clinical efficacy by increasing binding to FcγRIIIa, thereby enhancing ADCC activity (Dalle et al., 2011; Junttila et al., 2010). As with sialylated glycoforms, diseases associated with modulations in fucose levels on Fc glycans suggests strict regulation of Fc fucosylation; an example of this is fetal or neonatal alloimmune thrombocytopenia, in which IgG specific for human platelet antigens (HPA) have significantly diminished levels of fucosylated Fc glycans, with levels of afucosylated anti-HPA correlating with disease severity (Kapur et al., 2014).

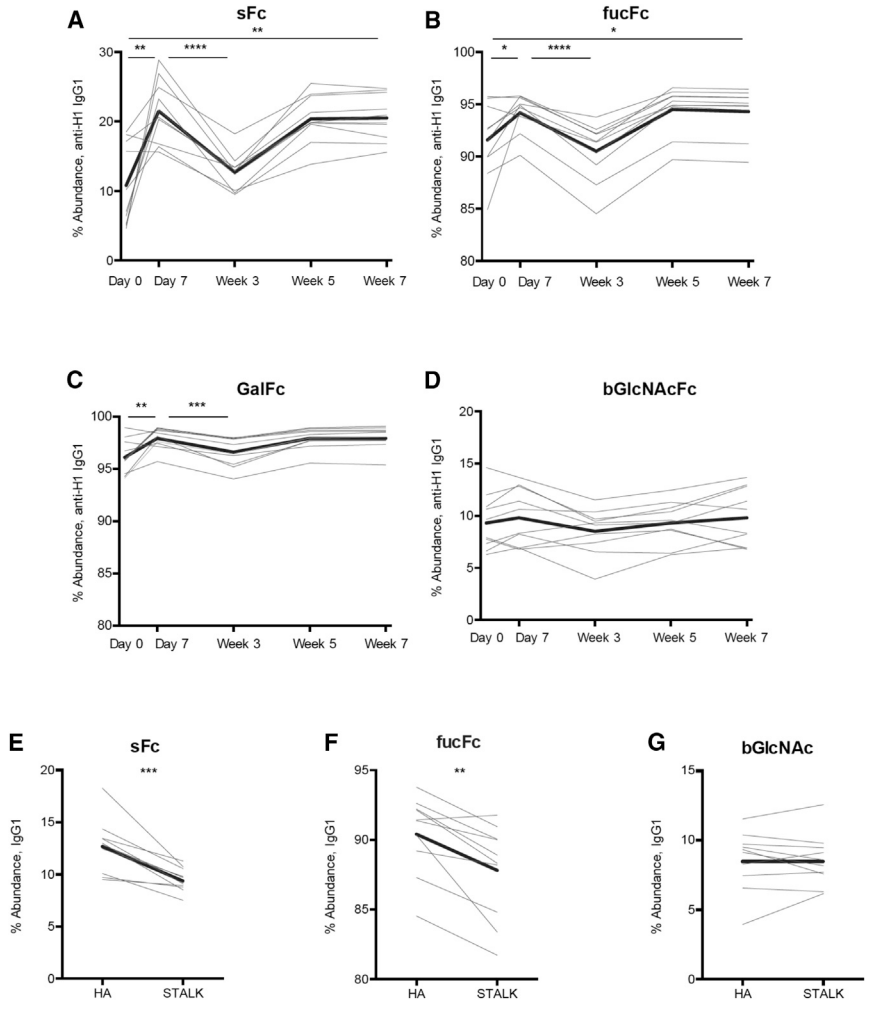

Figure 2. Regulation of Fc Glycan Composition Following TIV Vaccination

(A–D) Fc glycoforms on anti-H1 HA (Cal/09) IgG1 were analyzed. (A) Sialylated (sFc) and (B) fucosylated (fucFc) glycoforms were significantly elevated on day 7 post-vaccination. (C) Galactosylation (GalFc) levels were modulated to a small degree following vaccination. (D) Bisected GlcNAc (bGlcNAcFc) modifications were not regulated.

(E and F) Anti-HA (predominantly globular head-specific) and anti-HA stalk IgG1 differed significantly in Fc glycoform profile at week 3, with sialylated, fucosylated glycan levels highest on anti-HA IgG1 and lowest on stalk-specific IgG1.

(G) No difference in level of bisecting GlcNAc was observed. Bold line represents group mean in each panel.

*$p < 0.05$; **$p < 0.01$; ***$p < 0.001$; ****$p < 0.0001$ determined by two-tailed, paired Student's t tests. See also Figure S2.

RESULTS

Characterization of Fc Domain Structure on TIV-Elicited IgGs

Healthy adults were vaccinated with the 2012–2013 TIV. Sera were drawn at baseline (pre-vaccination), day 7, week 3, week 5, and week 7 following vaccination and antigen-specific IgGs were isolated for subsequent analysis of Fc glycan composition and IgG subclass (Figure S1A). At baseline, all subjects were positive for IgG against the H1 HA vaccine component, A/California/04/2009 (H1N1 virus), by H1 binding ELISA and the hemagglutination inhibition (HAI) test using homologous virus (Figures S2A and S2B). Baseline anti-H1 IgG was characterized for subclass distribution and Fc glycan composition (Figures 1B and 1E). Fc glycoforms on baseline anti-H1 IgG were predominantly neutral, with an inter-subject range of 66.3%–88.3%, bisecting GlcNAc moieties were present with a range of 6.2%–14.6%, sialylated glycoforms were present with a range of 4.6%–18.5%, and afucosylated glycans were present with a range of 4.27%–15.07% (Figure S2C). Anti-H1 IgG at baseline contained significantly more sFc and less fucosylated (fucFc) than total IgG, while subclass distribution was not different between H1-specific and total IgG (Figures S2D–S2F).

Following vaccination, modulations in the abundance of sFc glycoforms on H1-specific IgG were observed. sFc glycoforms were significantly elevated and at peak abundance by day 7 post-vaccination; this was mirrored by an increase in fucFc by day 7. sFc glycoforms and fucFc on anti-H1 IgG were consistently elevated above pre-vaccination levels through week 7 except for a significant dip at week 3 post-vaccination (Figures 2A and 2B).

Because galactosylation is a prerequisite for sialylation of the Fc glycan, the presence of galactose could be a limiting factor in

That Fc glycan modulation may result in autocrine B cell signaling through IC-FcR interactions, potentially directing the antibody response to vaccination, is suggested by the observations that Fc glycan composition can change following vaccination (Selman et al., 2012) and that sFc can bind CD23, the type II FcR expressed on activated B cells (Sondermann et al., 2013). The present study was designed to determine whether Fc structure within vaccine antigen-IgG ICs might be regulated as a mechanism of directing FcR-mediated processes involved in maturation of antibody responses. Our approach was to characterize modulations in the structural determinants of Fc domains (IgG subclass and Fc glycan composition) on IgGs elicited by administration of the trivalent influenza virus vaccine (TIV) in healthy subjects. Next, we performed a series of directed experiments to determine what role, if any, the modulations played in determining vaccine responses. Our results on the natural regulation of Fc domain structure during the evolution of protective vaccine responses suggest immunization strategies involving administration of ICs containing sFc to elicit broadly protective antibodies against influenza viruses.

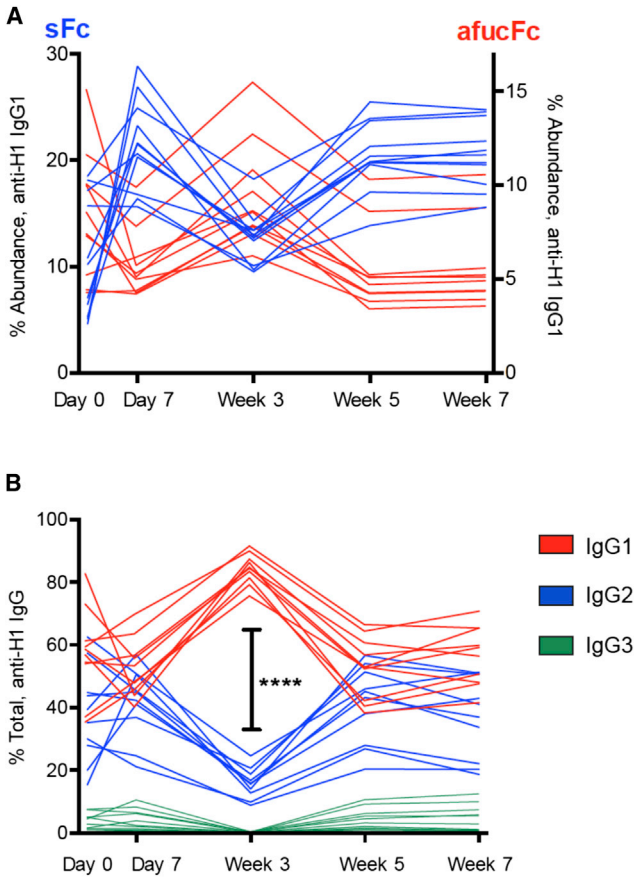

Figure 3. Modulations in Fc Domain Structure Favor Type II FcR Binding at Day 7 and Type I FcR Binding at Week 3 Post-Vaccination

(A) Fc glycoforms shift from type II FcR binding (high in sFc) at day 7 to type I FcR binding (high in afucFc content) by week 3.

(B) The activating FcR binding glycoform profile at week 3 was mirrored by a peak in IgG1 subclass. IgG4 was not in sufficient abundance to accurately quantify. *$p < 0.05$; **$p < 0.01$; ***$p < 0.001$; ****$p < 0.0001$ determined by the Tukey post hoc test.

See also Figure S3.

determining the abundance of sialic acid modifications. Analysis showed that galactose (GalFc) levels were modulated to a small, but statistically significant degree following vaccination, but that the overall abundance of galactosylated glycans was over 90% at every time point (Figure 2C). This was several fold higher than sialylated glycans, suggesting that galactosylation was not limiting and that modulations in sialylation were independently regulated. There was no apparent regulation of bisected GlcNac glycoforms (bGlcNAcFc) (Figure 2D).

In addition to regulation of Fc glycoforms over time following vaccination, analysis of HA-specific IgG from a single time point, week 3, revealed that specific Fc glycoforms can be linked to Fab specificity, possibly due to differential glycosylaytion by distinct IgG-producing B cell subsets such as plasmablasts (PB) and memory B cells. Anti-HA (predominantly globular head-specific) and anti-HA stalk IgG differed significantly in Fc glycoform profile, with sialylated, fucosylated glycan levels highest on total anti-HA IgG and lowest on anti-HA stalk IgG (Figures 2E and 2F and Figure S2E). No differences were observed in levels of bisecting GlcNAc (Figure 2G).

Day 7 post-vaccination was characterized by an increase in sFc on anti-H1 IgG, which would increase type II FcR binding by ICs. In contrast, week 3 post-vaccination was characterized by diminished sFc and elevated afucosylated Fc (afucFc), which would shift the signaling balance toward activating Type I FcRs (Figure 3A). This shift in Fc glycoform composition toward activating type I FcR signaling at week 3 was mirrored by modulations in subclass distribution of anti-H1 IgGs, from a median IgG1 abundance of 35.2% at baseline, to a median level of 75.18% by week 3 (Figure 3B).

Fc Glycoforms Present Following Vaccination Mirror Glycosyltransferase Expression in Activated B cell Subsets

Peak levels of sialylated and fucosylated Fc glycans at day 7 post-vaccination mirrored a peak in plasmablast (PB) abundance in the peripheral blood of our study subjects, in accordance with the well-described kinetics of plasmablast expansion that occurs following TIV administration (Figure S3A) (Wrammert et al., 2008). In addition, the amount of anti-H1 IgG produced during the early plasmablast response correlated with the change in sFc abundance on anti-HA IgG in the first 7 days following vaccination ($p = 0.0065$) (Figure S3B). These observations led us to hypothesize that sialylated, fucosylated Fc glycoforms may be produced, at least in part, by PB. Because the increase in relative abundance of afucFc and asialylated Fc glycoforms from day 7 to week 3 mirrored a small increase in peripheral memory B cells in our patient cohort (Figure S3C), as has been previously described (Pinna et al., 2009), we hypothesized that that those glycoforms may derive from memory B cells. Intracellular staining of PB and memory B cells for the relevant glycosyltransferases, ST6Gal1 and FUT8, revealed increased ST6Gal1 expression and non-significantly increased FUT8 expression in PB over memory B cells (Figures S3D and S3E). In addition, gene analysis of day 7 PB and memory B cells from six patients who received the 2009–10 TIV revealed elevated levels of *ST6Gal1* ($p = 0.06$) and *FUT8* ($p = 0.03$) in PB over memory B cells (Figures S3E and S3G), supporting the possible production of sialylated, fucosylated Fc glycans by PB and less sialylated, less fucosylated Fc glycans by memory cells. Unlike *ST6Gal1* and *FUT8, B4GALT1*, coding for a galactosyltransferase involved in Fc glycan modification, was not significantly elevated in PB (Figure S3H).

Sialylated Fc Abundance Predicts Influenza Virus Vaccine Efficacy, Defined by Change in HAI+ Titer Post-Vaccination

To investigate the significance of the regulated changes in Fc glycan composition following TIV vaccination, we assessed association of specific Fc glycoform abundance with change in hemagglutination inhibition titer (HAI), a commonly used measure of TIV efficacy. In particular, since the degree of HA-specific plasmablast expansion on day 7 post-vaccination has been observed to loosely correlate with vaccine response, we investigated any association between production of sialylated

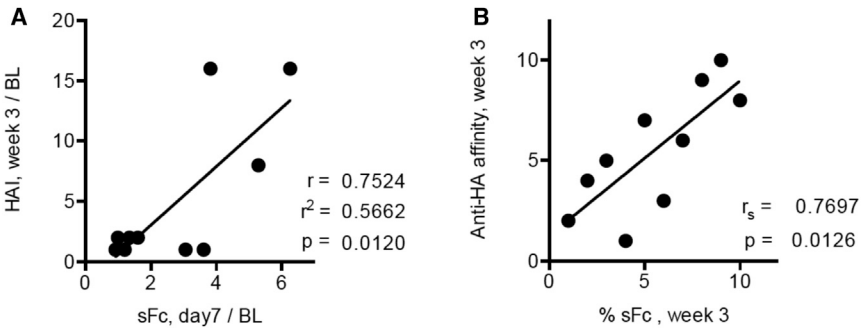

Figure 4. Sialylated Fc Abundance Predicts Influenza Virus Vaccine Efficacy

(A) Fold change in sFc on anti-HA IgG1 from baseline to day 7 post-vaccination (sFc, day7/BL) predicted fold change in HAI titer from baseline to week 3 (HAI, week 3/BL).

(B) Spearman's rank correlation: sFc abundance at week 3 post-vaccination (% sFc, week 3) predicted affinity of anti-HA IgG at week 3 (anti-HA affinity, week 3). Correlation analysis was used to determine the Pearson correlation coefficient (r) (following confirmation of normal distribution) and Spearman's rank correlation coefficient (r_s), linear regression was used to determine goodness of fit (r^2).

IgG on day 7 and vaccine efficacy as measured by HAI titer by week 3 (Nakaya et al., 2011; Wrammert et al., 2008). Indeed, the change in abundance of sialylated glycoforms on anti-HA IgG in the first week following vaccination was predictive of subsequent increase in HAI activity (Figure 4A). In addition, sialylated glycoform abundance predicted affinity of anti-HA IgG at week 3 post-vaccination (Figure 4B). These data suggested that the abundance of sialylated Fc glycoforms produced following TIV administration could regulate the quality of the overall vaccine response.

Sialylated Fc Glycoforms in ICs Trigger Upregulation of FcγRIIB on B Cells in a CD23-Dependent Manner

To determine the mechanisms by which sFc within immune complexes might modulate B cell activation, we studied the effects of sFc ICs on B cells in a variety of in vitro and in vivo assays. Pooled IgG from week 3 post-vaccination, either with native sFc levels (17.6% on anti-HA IgG) or neuraminidase treated to remove native sialic acids (asialylated) (Figure S4) was complexed with California/04/2009 (Cal/09) H1 HA protein to form sialylated or asialylated IC (sIC or aIC). These ICs were incubated with human CD19+ PBMCs and analysis after 24 hr incubation revealed increased expression of FcγRIIB, the inhibitory type I Fc receptor, on cells incubated with sIC but not aIC or HA protein alone (Figure 5A). Similarly, a recombinant anti-HA mAb, PY102 (Dinca et al., 1993), was expressed with sialylated Fc glycoforms (23.7% sFc), or in an asialylated form, and was mixed with A/PR8/1934 (PR8) H1 HA protein to form sIC or aIC. These mAb ICs were then incubated with BJAB cells and, consistent with the primary B cell assay, incubation with sICs, but not aIC or HA protein alone induced upregulation of FcγRIIB expression (Figure 5B).

Next, to determine how sialylated ICs might affect B cells in vivo, the human post-vaccination IgG/Cal/09 HA ICs (sIC and aIC) were used to prime mice, followed by HA protein boost 3 weeks later. Ten days post-boost, peripheral B cells were analyzed for FcγRIIB expression; antigen-specific peripheral B cells from mice primed with sIC showed increased expression of FcγRIIB, whereas mice primed with aICs showed no such elevation (Figure 5C). Similarly, sIC or aIC made from mAb PY102 and PR8 HA protein were used to vaccinate mice; 3 days post-vaccination, germinal center B cells from mice immunized with sIC, but not aIC or HA alone had increased FcγRIIB expression (Figure 5D). Because CD23 is the only type II FcR expressed on B cells, we next determined whether upregulation of FcγRIIB was dependent on CD23 expression. CD23-deficient mice did not display upregulation of FcγRIIB on germinal center B cells, demonstrating that sICs acted through CD23 to trigger upregulation of B cell FcγRIIB (Figure 5D).

IgG Elicited by Sialylated ICs Are Higher Affinity for Antigen

Increased FcγRIIB expression is known to elevate thresholds for selection of B cells based on affinity of BCR, thus, we characterized the affinity of anti-HA IgG elicited by immunization with sICs (Bolland and Ravetch, 2000; Pearse et al., 1999). The affinity of IgGs elicited by human post-vaccination IgG/Cal/09 HA ICs was measured using an affinity ELISA assay that was modified from a nitrophenyl system for evaluation of anti-HA IgGs; this assay measures the ratio of high-affinity to all-affinity binding IgGs (Herzenberg et al., 1980; Kaisho et al., 1997). The affinity for the Cal/09 HA1 subunit was also evaluated using a method that measures the quantity of IgG remaining bound following treatment with 7M urea (Verma et al., 2012). IgGs elicited by the sIC priming protocol had significantly higher affinity for Cal/09 HA1 (primarily globular head), the highly conserved stalk domain of the H1 subtype HA protein, and for the complete Cal/09 HA glycoprotein (Figures 6A–6D). Consistent with the lack of FcγRIIB upregulation using the sIC priming protocol in CD23-deficient mice (Figure 5D), elevated affinity of elicited IgGs was not achieved in CD23-deficient mice (Figure 6D). The affinity of IgGs elicited by mAb PY102/PR8 HA ICs for the PR8 H1 protein or the PR8 stalk domain was assessed using surface plasmon resonance (SPR) analysis (Verma et al., 2012). The polyclonal serum antibody dissociation off-rate for anti-HA IgG from mice primed with sIC was found to be approximately 10- to 20-fold lower than that of IgG from mice primed with aIC- or CD23-deficient mice that received sIC (Figure 6E).

Higher Affinity IgGs Mediate Broad Protection against H1N1 Influenza Viruses

To determine any functional significance associated with increasing affinity of anti-HA IgGs, we tested pooled IgG from mice primed with polyclonal, human, post-vaccination IgG/Cal/09 HA IC or HA alone for protective activity (pools were derived

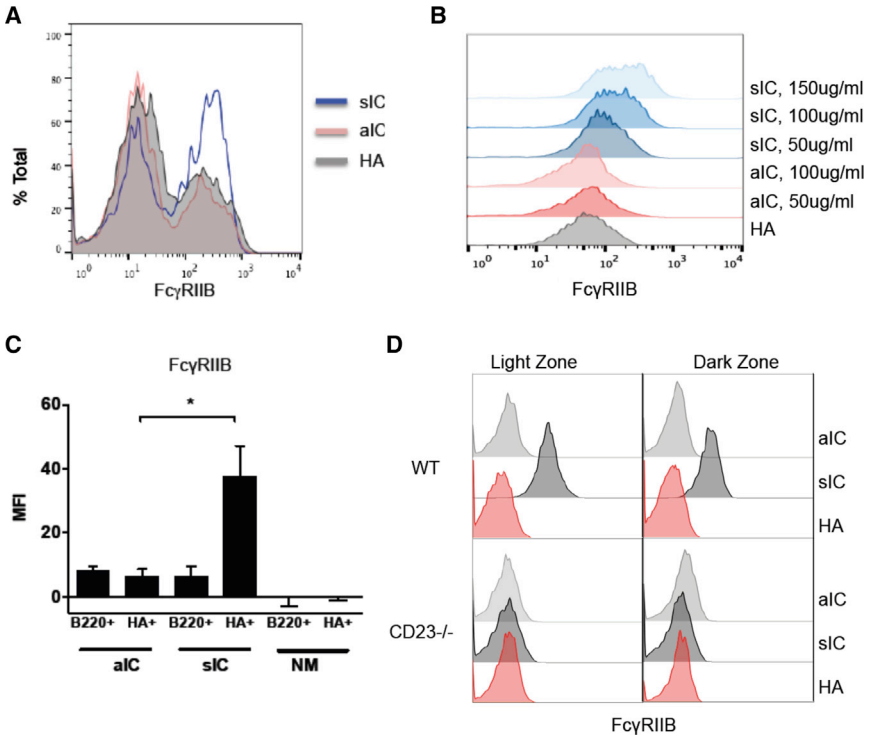

Figure 5. sFc in ICs Trigger Upregulation of FcγRIIb on B Cells

(A) sIC or aIC were generated from pooled, post-vaccination human IgG and Cal/09 HA protein. Human, $CD19^+$ PBMCs were incubated with sIC, aIC or HA protein alone. FACS analysis following incubation revealed an increased number of cells expressing FcγRIIB with sIC but not with aIC or HA incubation.

(B) sIC or aIC were generated from PY102 and PR8 HA protein. BJAB B cells were incubated with sIC, aIC or HA at the indicated IC concentrations. Incubation with sIC but not aIC or HA alone increased FcγRIIB expression on B cells.

(C) Antigen-specific (HA-specific) peripheral B cells from mice primed with sIC showed increased FcγRIIB, whereas mice primed with aICs or naive mice (NM) showed no elevation in peripheral B cell FcγRIIB expression. Five mice per group. Data are represented as mean ± SD.

(D) Splenic B cells in the light and dark zones of the germinal center from mice primed with sIC, but not aIC or mock showed increased expression of FcγRIIB. Increased FcγRIIB expression was not present in CD23 knockout mice (CD23−/−) primed with sIC.

All panels are representative of experiments performed in duplicate or triplicate. See also Figure S4.

from sera tested in Figure 6). IgG pools had equivalent HAI endpoint titers using virus expressing the homologous HA used for vaccination (A/Netherlands/602/2009) (Figure S5A) and equivalent binding activity for Cal/09 or Cal/09 stalk proteins (Figures S5B–S5G). For challenge experiments, virus was pre-incubated with purified IgG prior to intranasal infection; thus, weight loss was a function of dose of infectious virus remaining after incubation with IgG pools. On challenge, equivalent protection was observed against the H1N1 virus A/Netherlands/602/2009, which expresses the homologous HA used for vaccination (Figures 7A and 7B). In contrast, when we evaluated only anti-stalk IgGs for protective activity using a virus that expresses a chimeric hemagglutinin molecule (cH5/1) comprised of the highly conserved H1 stalk domain and an irrelevant head subtype domain (H5), we observed a difference in protective potency of the IgG pools. Only the higher affinity IgGs elicited by priming with sIC conferred anti-stalk-mediated protection (Figures 7C and 7D).

Next, equivalent challenge experiments were performed using IgG from mice immunized with mAb PY102/PR8 HA IC (sIC in wild-type mice, sIC in CD23-deficient mice or aIC) or PR8 HA alone. Purified IgG pools had equivalent binding titers for PR8 HA (Figure S5H). Mice were challenged with A/PR8/1934 virus, which expresses the homologous H1 HA used for vaccination and, as before, complete protection was achieved with all IgG pools (Figures 7E and 7F). In contrast, only IgG elicited by sIC protected mice from challenge with either A/FM/1/1947 H1N1 virus or A/Netherlands/602/2009 H1N1 virus (Figures 7G–7J), demonstrating breadth of protection conferred by higher affinity IgG elicited by sIC.

DISCUSSION

That sFc produced during the early plasmablast response was found to correlate with subsequent production of HAI+ antibody suggested a possible requirement for immunomodulatory type II FcR signaling in the ontogeny of protective TIV responses. Further experiments demonstrated that sFc within immune complexes triggered upregulation of B cell FcγRIIb, thus modulating the selection of B cells in favor of those expressing higher affinity BCR. Our studies suggest a model whereby TIV vaccination triggers plasmablast expansion and production of sFc IgG. Immune complexes formed with sFc IgG signal through the type II FcR CD23 on activated B cells, triggering increased FcγRIIb expression. This results in an elevation of threshold for BCR affinity that is required for B cell survival and, ultimately, production of higher affinity, more potently protective IgG (Figure S6).

Several studies, including the present, have found that baseline titer of anti-HA IgG correlates negatively with the magnitude of TIV response, so that low baseline titer predicts greater vaccine response (Figure S7A) (Beyer et al., 1996; Sasaki et al., 2008; Tsang et al., 2014). Low baseline anti-HA titer also predicts greater plasmablast frequency (Tsang et al., 2014) and predicted increased production of sFc glycoforms by day 7 post-vaccination (Figure S7B). Overall, low baseline anti-HA IgG predicts large plasmablast expansion and abundant production of sialylated glycoforms within the week following vaccination, resulting in a greater change in HAI+ IgG. Of note, greater production of sialylated Fc glycoforms by day 7 could also be predicted by baseline sialylated Fc abundance, with lower baseline sialylated

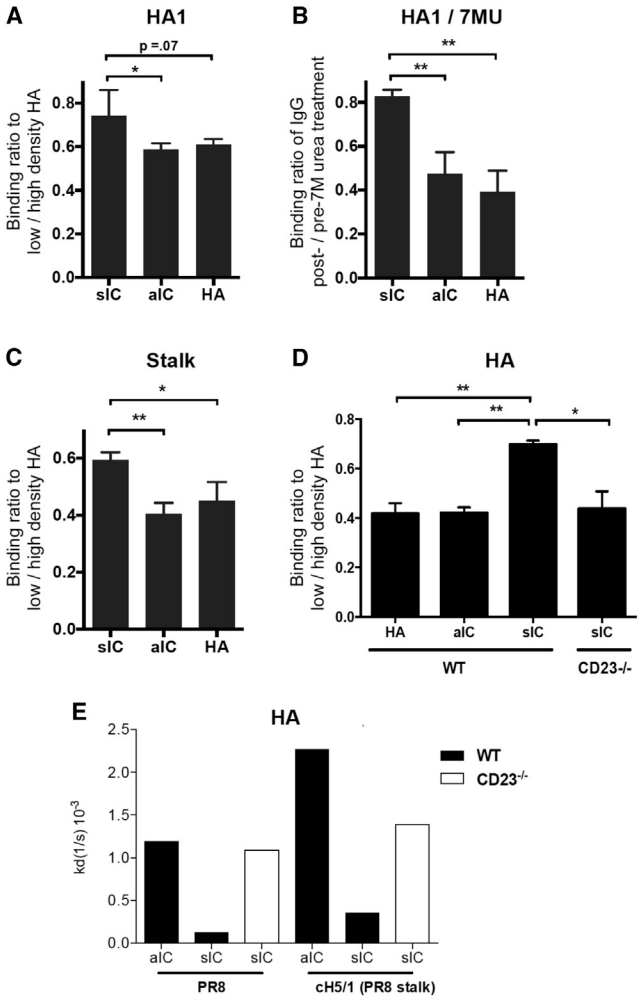

Figure 6. sFc in ICs Elicit Higher Affinity IgG

(A–E) IgGs elicited by sIC had significantly higher affinity for (A and B) the globular head, (C) the stalk domain of the HA protein, and (D) the wild-type Cal/09 H1 subtype HA protein when compared with the affinities of IgG elicited by aIC or HA alone. Only wild-type mice and not CD23-deficient mice generated higher affinity, anti-HA IgGs in response to an immunization protocol with sIC priming. Affinity measurement in (B) was determined by 7M urea ELISA, expressed as IgG bound to HA following 7M urea treatment/IgG bound without 7M urea treatment; affinity measurements in (A), (C) and (D) were determined by ELISA, expressed as binding ratio to low density/high density of plate-bound HA protein. Data are represented as mean ± SEM (E) SPR analysis of off-rate constant of polyclonal IgG elicited by mAb PY102-HA ICs in wild-type or CD23−/− mice. sIC priming protocol in wild-type mice elicited approximately 10- to 20-fold higher affinity IgGs over aIC priming or sIC priming in CD23−/− mice.

*p < 0.05; **p < 0.01; ***p < 0.001; ****p < 0.0001 determined by two-tailed Student's t test.

glycoform abundance correlating with greater subsequent sFc production (Figure S7C).

The finding that protective anti-stalk IgGs can be elicited by sialylated ICs is significant as anti-stalk IgGs can mediate broad protection against antigenically distinct influenza viruses (Krammer et al., 2013; Pica et al., 2012; Wang et al., 2010). One practical application suggested by the observation that sialylated immune complexes can drive selection of higher affinity B cells, would be to use this as a strategy to selectively elicit higher affinity anti-stalk IgGs, thereby generating broader and more potent anti-HA responses. The finding also suggests an affinity requirement for protective anti-stalk IgGs that is not present for globular head-specific antibodies; higher affinity may be required of anti-stalk IgGs in order to restrict the conformation change in the HA that occurs at low pH, thus preventing fusion of the viral envelope with the host cell.

Because balanced FcR signaling is a requirement for generation of specific immune responses, strict regulation of Fc domain structure within ICs must occur (Bolland and Ravetch, 2000; Fukuyama et al., 2005). We show that this regulation occurs through synchronized modulations in determinants of Fc domain structure following exposure to antigen. The changes observed, over the weeks following vaccination, would regulate type I and type II FcR signaling within B cell follicles where antigen can be retained for months and even years following exposure (Nossal, 1992). PB that expand following TIV are a possible source of sFc IgG observed at day 7, while memory B cells may contribute to production of the less fucosylated, less sialylated Fc glycoforms observed at week 3. Production of less fucosylated, less sialylated glycoforms by memory B cells may be supported by the finding that these glycoforms are present with greater abundance on IgGs specific for the highly conserved stalk domain of the HA. A shift toward Fc domains with increased type I FcR binding at week 3 was pronounced in both Fc glycoform and IgG subclass distribution; a possible function of the increased activating type I FcR signaling may be to provide an adaptive mechanism for enhancing phagocyte activity during prolonged antigen exposure or infection.

Further studies will be required to dissect the undoubtedly complex role of Fc glycoform modulations during evolution of humoral immune responses, including both sialylated and low-fucose forms, as they are likely involved in regulation of multiple processes within the germinal center in addition to B cell activation and selection.

EXPERIMENTAL PROCEDURES

Clinical Studies

The 2012–2013 TIV vaccination study was conducted at the Rockefeller University Hospital in New York City in accordance with a protocol approved by the Institutional Review Board of Rockefeller University (protocol #TWA-0804), in compliance with guidelines of the International Conference on Harmonization Good Clinical Practice guidelines, and was registered on www.clinicaltrials.gov (NCT01967238). Samples were drawn from ten healthy adult volunteers (Figure S1). B cells analyzed for gene expression derived from six donors as part of a study approved by the Emory University institutional review board (IRB #00022916). Healthy volunteers received the 2009–2010 trivalent inactivated influenza vaccine. All samples were processed within 30 min of being drawn; sera and PBMCs were stored at −80°C and were thawed once prior to analysis.

Recombinant Proteins and Generation of Immune Complexes

Recombinant anti-HA mAb PY102 was expressed as a human IgG1 in 293T cells stably expressing human ST6GAL1 and B4GALT1 and purified using protein G chromatography as previously described (Bournazos et al., 2014). HA proteins were expressed in a baculovirus system as previously described (Pica et al., 2012). ICs were formed by incubation of molar ratio 30:1 (purified,

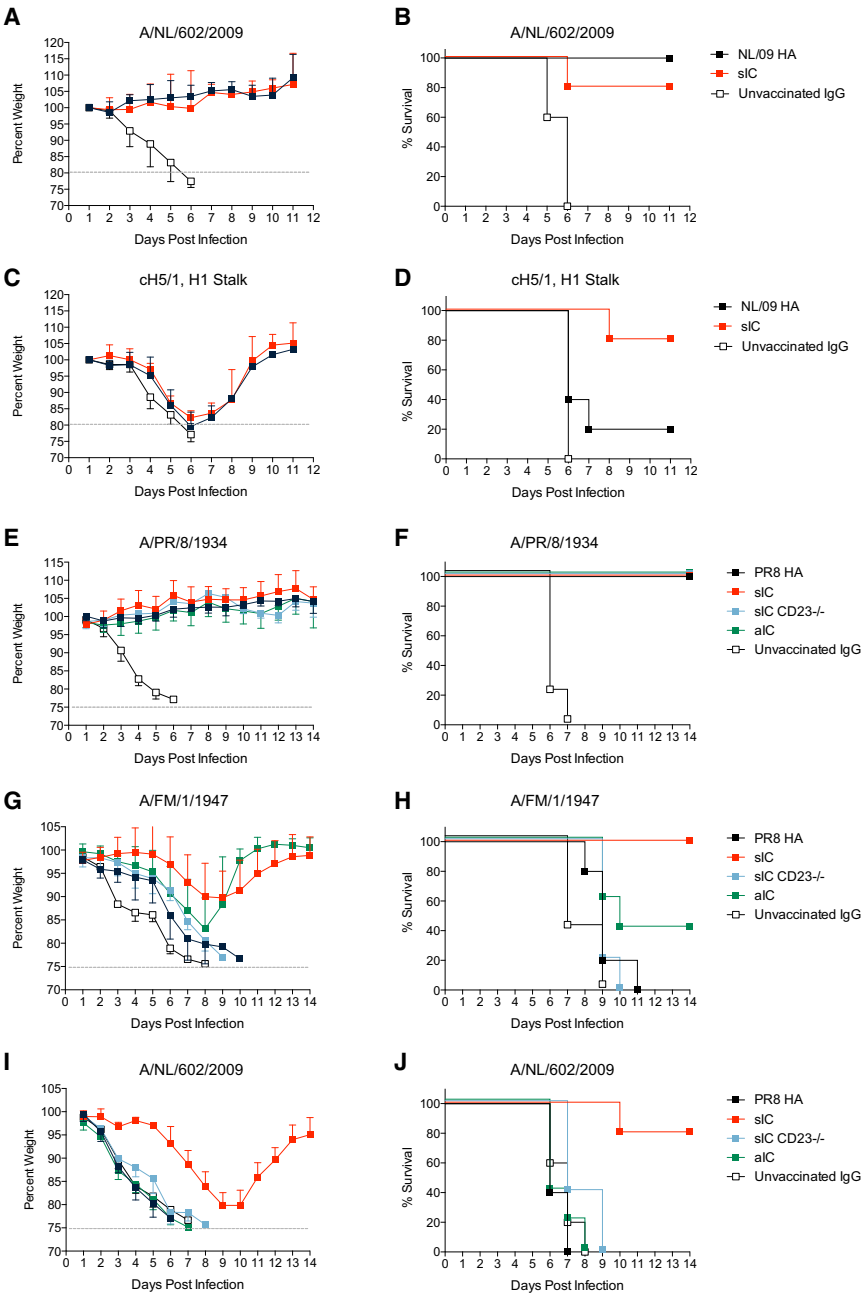

Figure 7. Immunization with sIC Elicits IgGs with Greater Breadth of Protective Potency against Distinct H1 Influenza Viruses

(A and B) Purified IgGs were pooled from mice primed with sIC (Cal/09 HA) or Cal/09 HA alone followed by two boost immunizations of Cal/09 HA. IgG from either pool conferred equivalent protection against A/Netherlands/602/2009 (H1N1).

(C and D) In contrast, only IgGs elicited by priming with sICs conferred anti-stalk-mediated protection against the chimeric cH5/1 virus that expresses an HA with an H1 stalk domain and an H5 subtype globular head.

(E and F) Purified IgGs were pooled from mice primed with monoclonal PY102-PR8 HA ICs or PR8 HA alone. ICs used were: sIC in wild-type mice, sIC in CD23−/− mice or aIC in wild-type mice. IgG from all pools conferred equivalent protection against A/PR8/1934 virus (H1N1).

(G–J) In contrast, only IgG elicited by sIC protected mice from challenge with (G and H) A/FM/1/1947 (H1N1) virus or (I and J) A/Netherlands/602/2009 virus.

The number of animals used was 5–10 per group in each experiment. See also Figure S5.

polyclonal human IgG) or 3:1 (mAb PY102) IgG:HA trimer for 1 hr at 4°C. These IgG:HA ratios were designed to generate 1:1 complexes with IgG and HA monomer; a 30:1 ratio was used for polyclonal IgG:HA based on a predicted anti-HA frequency of 1 in 10 IgGs post-vaccination. IgG subclass and Fc glycan composition were determined by mass spectrometry; size of ICs was determined by size exclusion chromatography (See Supplemental Experimental Procedures for detailed protocols).

Fc Glycan Analysis

IgGs were isolated from serum by protein G purification. HA-specific IgGs were isolated on agarose resin (Pierce) coupled to HA protein. Total anti-H1 HA IgGs were captured on Cal/09-coupled resin while anti-H1 stalk proteins were captured using resin coupled to a chimeric hemagglutinin protein expressing the Cal/09 stalk and an H5 subtype globular head domain. IgG Fc-associated glycans were analyzed by mass spectrometry following tryptic digestion of purified IgG or on-bead IgG. Relative IgG subclass distribution was determined by mass spectrometric quantification of subclass-specific tryptic peptides. IgG4 was not in sufficient abundance to accurately quantify. See Supplemental Experimental Procedures for detailed mass spectrometric methods.

ELISAs

HA ELISAs were performed as described previously (Wang et al., 2010). Negative control (naive mouse serum or binding values of human IgGs on the irrelevant protein BSA) values were subtracted from readings given by test samples. Study subjects were determined to have positive IgG binding titers when binding was five times above background. For affinity ELISAs, sera diluted 1:200 were incubated on plates coated with 1ug/ml HA protein (low density) or 6 μg/ml HA (high density). The affinity of HA-specific IgG was expressed as a ratio of binding to low-density:high-density HA-coated plates. This method was adapted from the well-established assay used for measurement of polyclonal anti-nitrophenyl-hapten affinity (Herzenberg et al., 1980). The 7M urea affinity ELISA was performed as previously described (Verma et al., 2012). HA1 protein (Sino Biological), chimeric cH5/1 protein (head domain derived from H5N1 strain A/Viet Nam/1203/04 and a stalk domain derived from H1N1 strain A/Puerto Rico/8/34) or Cal/09 or PR8 full-length HA proteins were used.

Hemagglutination Inhibition Assay

Sera were tested in a standard hemagglutination inhibition assay, as previously described (WHO, 2002).

Surface Plasmon Resonance Analysis

The binding properties of serum antibodies were analyzed by SPR (Biacore T-200. GE Healthcare). Protein G-purified serum IgG from vaccinated mice was immobilized to the surface of a CM5 sensor chip (GE Healthcare) using

amine coupling chemistry at a density of 1,000 RU. Varying concentration (1 nM–50 nM) of either PR8-HA or cH5/1 HA were injected sequentially over flowcells of the sensor chip. Samples were fit to heterogeneous ligand binding model and the off-rate constant (kd/s) was calculated.

In Vitro Studies

Human, $CD19^+$ PBMCs or BJAB cells were treated with IL-4 (200 ng/ml) and CD40L (5 μg/ml) to increase surface expression of CD23 prior to incubation with IC.

In Vivo Studies

All mice were maintained in a specific-pathogen–free facility at the Rockefeller University and all studies were approved by the Rockefeller University Institutional Animal Care and Use Committee.

Polyclonal IC immunization: For mouse immunizations using human serum-derived ICs, A/California/04/2009 HA protein (10 μg) was delivered alone, or in complex with pooled, protein G-purified, week 3 post-vaccination IgG from vaccinated subjects. As control, asialylated IgG was prepared by treatment of IgG with α2-3,6,8 Neuraminidase (New England Biolabs) as described (Anthony et al., 2011). Mice previously administered ICs or HA in PBS were boosted, intraperitoneally, at 3 week intervals, with 10 μg HA in adjuvant (complete/incomplete Freund's or Alum).

For in vivo neutralization studies, anesthetized mice (female C57BL/6J; 6- to 8-week-old) were infected intranasally with 5 mLD50 of the A/Netherlands/602/09 (H1N1) or $cH5/1_{PR8}N1_{PR8}$ virus (the HA contains a head domain derived from H5N1 strain A/Viet Nam/1203/04 and a stalk domain derived from H1N1 strain A/Puerto Rico/8/34—generated as described in Hai et al., 2012). IgGs from vaccinated mice were purified from pooled sera using protein G (GE Healthcare) and mixed with virus prior to intranasal infections. For the Netherlands/09 challenge, 10 μg/ml IgG was mixed with virus, for the cH5/1 challenge, 200 μg/ml IgG was used. Mouse body weight was recorded daily, and death was determined by a 20% body weight loss threshold.

Monoclonal IC immunizations: For PY102 mAb immunizations, 20 μg PR8 HA and 50 μg PY102 or 20 μg PR8 HA alone was delivered intravenously to 6-week-old wild-type or $CD23^{-/-}$ BALB/c mice. Boosts were administered as described above. For challenge studies, mice were anesthetized and infected as described above. A mixture of mouse-adapted virus (A/PR8/1934 (H1N1), A/FM/1/1947 (H1N1) or A/Netherlands/602/09 (H1N1) and purified polyclonal IgG (75 μg/ml) from vaccinated mice was pre-incubated at room temperature for 30 min. Six- to eight-week old female BALB/c mice were then infected with 5 mLD50 of virus. Mice were weighed daily to monitor morbidity and animals that exceeded 25% weight loss were euthanized.

Statistical Analysis

All data were analyzed in Prism 6 (GraphPad). Results from multiple experiments are presented as mean ± SEM. Correlation analysis was used to determine the Pearson correlation coefficient, r. Linear regression was used to determine goodness of fit, R^2.

Two tail paired/unpaired Student's t tests or ANOVA followed by Tukey post hoc analysis were performed to assess differences in the mean values of quantitative variables. Non parametric tests of significance were performed if normal distribution could not be assessed or if populations were not normally distributed.

SUPPLEMENTAL INFORMATION

Supplemental Information includes Supplemental Experimental Procedures and seven figures and can be found with this article online at http://dx.doi.org/10.1016/j.cell.2015.06.026.

AUTHOR CONTRIBUTIONS

T.T.W. and S.J.S. designed the clinical study. T.T.W., J.M. and J.V.R. designed research and analyzed data. T.T.W., J.M., G.S.T., S.B. and C.W.D. conducted experiments. R.A. and P.P. provided intellectual input. F.K. contributed analytical reagents and intellectual input. T.T.W. and J.V.R. wrote the manuscript.

ACKNOWLEDGMENTS

We thank the Rockefeller University Hospital and all hospital staff involved in conducting the clinical study, in particular, Marina Caskey for helpful discussions, Noreen Buckley and Arlene Hurley for assistance in several aspects of protocol implementation and helpful discussions, and Joel Correa da Rosa for statistical assistance. We thank Sheng Zhang at the Cornell Proteomics and Mass Spectrometry Facility for helpful discussions and Robert Sherwood at the Cornell Proteomics and Mass Spectrometry Facility for helpful discussions and excellent technical support. T.T.W. thanks Barry Coller and the Rockefeller University KL2 Clinical Scholars Program for training and support. Research reported in this publication was supported by the National Institute of Allergy And Infectious Diseases of the NIH under Award Number U19AI111825 (J.V.R.) and U19AI109946 (P.P.). The content is solely the responsibility of the authors and does not necessarily represent the official views of the NIH. T.T.W. was supported as a Rockefeller University Clinical Scholar in part by the Iris and Junming Le Foundation, the Rockefeller University Center for Clinical and Translational Science grant # UL1 TR000043 from the National Center for Advancing Translational Sciences, NIH and the Clinical and Translational Science Award program. F.K. was supported in part by the Centers of Excellence for Influenza Research and Surveillance, contract # HHSN266200700010C. Support and infrastructure were also provided by The Rockefeller University.

Received: December 1, 2014
Revised: March 13, 2015
Accepted: May 11, 2015
Published: July 2, 2015

REFERENCES

Ahmed, A.A., Giddens, J., Pincetic, A., Lomino, J.V., Ravetch, J.V., Wang, L.X., and Bjorkman, P.J. (2014). Structural characterization of anti-inflammatory immunoglobulin G Fc proteins. J. Mol. Biol. *426*, 3166–3179.

Anthony, R.M., and Ravetch, J.V. (2010). A novel role for the IgG Fc glycan: the anti-inflammatory activity of sialylated IgG Fcs. J. Clin. Immunol. *30* (1), S9–S14.

Anthony, R.M., Nimmerjahn, F., Ashline, D.J., Reinhold, V.N., Paulson, J.C., and Ravetch, J.V. (2008a). Recapitulation of IVIG anti-inflammatory activity with a recombinant IgG Fc. Science *320*, 373–376.

Anthony, R.M., Wermeling, F., Karlsson, M.C., and Ravetch, J.V. (2008b). Identification of a receptor required for the anti-inflammatory activity of IVIG. Proc. Natl. Acad. Sci. USA *105*, 19571–19578.

Anthony, R.M., Kobayashi, T., Wermeling, F., and Ravetch, J.V. (2011). Intravenous gammaglobulin suppresses inflammation through a novel T(H)2 pathway. Nature *475*, 110–113.

Beyer, W.E., Palache, A.M., Sprenger, M.J., Hendriksen, E., Tukker, J.J., Darioli, R., van der Water, G.L., Masurel, N., and Osterhaus, A.D. (1996). Effects of repeated annual influenza vaccination on vaccine sero-response in young and elderly adults. Vaccine *14*, 1331–1339.

Bolland, S., and Ravetch, J.V. (2000). Spontaneous autoimmune disease in Fc(gamma)RIIB-deficient mice results from strain-specific epistasis. Immunity *13*, 277–285.

Bournazos, S., Klein, F., Pietzsch, J., Seaman, M.S., Nussenzweig, M.C., and Ravetch, J.V. (2014). Broadly neutralizing anti-HIV-1 antibodies require Fc effector functions for in vivo activity. Cell *158*, 1243–1253.

Dalle, S., Reslan, L., Besseyre de Horts, T., Herveau, S., Herting, F., Plesa, A., Friess, T., Umana, P., Klein, C., and Dumontet, C. (2011). Preclinical studies on the mechanism of action and the anti-lymphoma activity of the novel anti-CD20 antibody GA101. Mol. Cancer Ther. *10*, 178–185.

de Man, Y.A., Dolhain, R.J., and Hazes, J.M. (2014). Disease activity or remission of rheumatoid arthritis before, during and following pregnancy. Curr. Opin. Rheumatol. *26*, 329–333.

Dinca, L., Neuwirth, S., Schulman, J., and Bona, C. (1993). Induction of antihemagglutinin antibodies by polyclonal antiidiotype antibodies. Viral Immunol. *6*, 75–84.

Espy, C., Morelle, W., Kavian, N., Grange, P., Goulvestre, C., Viallon, V., Chéreau, C., Pagnoux, C., Michalski, J.C., Guillevin, L., et al. (2011). Sialylation levels of anti-proteinase 3 antibodies are associated with the activity of granulomatosis with polyangiitis (Wegener's). Arthritis Rheum. *63*, 2105–2115.

Ferrara, C., Grau, S., Jäger, C., Sondermann, P., Brünker, P., Waldhauer, I., Hennig, M., Ruf, A., Rufer, A.C., Stihle, M., et al. (2011). Unique carbohydrate-carbohydrate interactions are required for high affinity binding between FcgammaRIII and antibodies lacking core fucose. Proc. Natl. Acad. Sci. USA *108*, 12669–12674.

Fukuyama, H., Nimmerjahn, F., and Ravetch, J.V. (2005). The inhibitory Fcgamma receptor modulates autoimmunity by limiting the accumulation of immunoglobulin G+ anti-DNA plasma cells. Nat. Immunol. *6*, 99–106.

Hai, R., Krammer, F., Tan, G.S., Pica, N., Eggink, D., Maamary, J., Margine, I., Albrecht, R.A., and Palese, P. (2012). Influenza viruses expressing chimeric hemagglutinins: globular head and stalk domains derived from different subtypes. J. Virol. *86*, 5774–5781.

Herzenberg, L.A., Black, S.J., Tokuhisa, T., and Herzenberg, L.A. (1980). Memory B cells at successive stages of differentiation. Affinity maturation and the role of IgD receptors. J. Exp. Med. *151*, 1071–1087.

Hodoniczky, J., Zheng, Y.Z., and James, D.C. (2005). Control of recombinant monoclonal antibody effector functions by Fc N-glycan remodeling in vitro. Biotechnol. Prog. *21*, 1644–1652.

Junttila, T.T., Parsons, K., Olsson, C., Lu, Y., Xin, Y., Theriault, J., Crocker, L., Pabonan, O., Baginski, T., Meng, G., et al. (2010). Superior in vivo efficacy of afucosylated trastuzumab in the treatment of HER2-amplified breast cancer. Cancer Res. *70*, 4481–4489.

Kaisho, T., Schwenk, F., and Rajewsky, K. (1997). The roles of gamma 1 heavy chain membrane expression and cytoplasmic tail in IgG1 responses. Science *276*, 412–415.

Kaneko, Y., Nimmerjahn, F., and Ravetch, J.V. (2006). Anti-inflammatory activity of immunoglobulin G resulting from Fc sialylation. Science *313*, 670–673.

Kapur, R., Kustiawan, I., Vestrheim, A., Koeleman, C.A., Visser, R., Einarsdottir, H.K., Porcelijn, L., Jackson, D., Kumpel, B., Deelder, A.M., et al. (2014). A prominent lack of IgG1-Fc fucosylation of platelet alloantibodies in pregnancy. Blood *123*, 471–480.

Krammer, F., Pica, N., Hai, R., Margine, I., and Palese, P. (2013). Chimeric hemagglutinin influenza virus vaccine constructs elicit broadly protective stalk-specific antibodies. J. Virol. *87*, 6542–6550.

Morell, A., Terry, W.D., and Waldmann, T.A. (1970). Metabolic properties of IgG subclasses in man. J. Clin. Invest. *49*, 673–680.

Nakaya, H.I., Wrammert, J., Lee, E.K., Racioppi, L., Marie-Kunze, S., Haining, W.N., Means, A.R., Kasturi, S.P., Khan, N., Li, G.M., et al. (2011). Systems biology of vaccination for seasonal influenza in humans. Nat. Immunol. *12*, 786–795.

Nossal, G.J. (1992). The molecular and cellular basis of affinity maturation in the antibody response. Cell *68*, 1–2.

Pearse, R.N., Kawabe, T., Bolland, S., Guinamard, R., Kurosaki, T., and Ravetch, J.V. (1999). SHIP recruitment attenuates Fc gamma RIIB-induced B cell apoptosis. Immunity *10*, 753–760.

Pica, N., Hai, R., Krammer, F., Wang, T.T., Maamary, J., Eggink, D., Tan, G.S., Krause, J.C., Moran, T., Stein, C.R., et al. (2012). Hemagglutinin stalk antibodies elicited by the 2009 pandemic influenza virus as a mechanism for the extinction of seasonal H1N1 viruses. Proc. Natl. Acad. Sci. USA *109*, 2573–2578.

Pincetic, A., Bournazos, S., DiLillo, D.J., Maamary, J., Wang, T.T., Dahan, R., Fiebiger, B.M., and Ravetch, J.V. (2014). Type I and type II Fc receptors regulate innate and adaptive immunity. Nat. Immunol. *15*, 707–716.

Pinna, D., Corti, D., Jarrossay, D., Sallusto, F., and Lanzavecchia, A. (2009). Clonal dissection of the human memory B-cell repertoire following infection and vaccination. Eur. J. Immunol. *39*, 1260–1270.

Sasaki, S., He, X.S., Holmes, T.H., Dekker, C.L., Kemble, G.W., Arvin, A.M., and Greenberg, H.B. (2008). Influence of prior influenza vaccination on antibody and B-cell responses. PLoS ONE *3*, e2975.

Scherer, H.U., van der Woude, D., Ioan-Facsinay, A., el Bannoudi, H., Trouw, L.A., Wang, J., Häupl, T., Burmester, G.R., Deelder, A.M., Huizinga, T.W., et al. (2010). Glycan profiling of anti-citrullinated protein antibodies isolated from human serum and synovial fluid. Arthritis Rheum. *62*, 1620–1629.

Selman, M.H., de Jong, S.E., Soonawala, D., Kroon, F.P., Adegnika, A.A., Deelder, A.M., Hokke, C.H., Yazdanbakhsh, M., and Wuhrer, M. (2012). Changes in antigen-specific IgG1 Fc N-glycosylation upon influenza and tetanus vaccination. Mol. Cell. Proteomics *11*, 014563.

Shields, R.L., Lai, J., Keck, R., O'Connell, L.Y., Hong, K., Meng, Y.G., Weikert, S.H., and Presta, L.G. (2002). Lack of fucose on human IgG1 N-linked oligosaccharide improves binding to human Fcgamma RIII and antibody-dependent cellular toxicity. J. Biol. Chem. *277*, 26733–26740.

Shinkawa, T., Nakamura, K., Yamane, N., Shoji-Hosaka, E., Kanda, Y., Sakurada, M., Uchida, K., Anazawa, H., Satoh, M., Yamasaki, M., et al. (2003). The absence of fucose but not the presence of galactose or bisecting N-acetylglucosamine of human IgG1 complex-type oligosaccharides shows the critical role of enhancing antibody-dependent cellular cytotoxicity. J. Biol. Chem. *278*, 3466–3473.

Sondermann, P., Pincetic, A., Maamary, J., Lammens, K., and Ravetch, J.V. (2013). General mechanism for modulating immunoglobulin effector function. Proc. Natl. Acad. Sci. USA *110*, 9868–9872.

Tomana, M., Schrohenloher, R.E., Koopman, W.J., Alarcón, G.S., and Paul, W.A. (1988). Abnormal glycosylation of serum IgG from patients with chronic inflammatory diseases. Arthritis Rheum. *31*, 333–338.

Tsang, J.S., Schwartzberg, P.L., Kotliarov, Y., Biancotto, A., Xie, Z., Germain, R.N., Wang, E., Olnes, M.J., Narayanan, M., Golding, H., et al.; Baylor HIPC Center; CHI Consortium (2014). Global analyses of human immune variation reveal baseline predictors of postvaccination responses. Cell *157*, 499–513.

Umaña, P., Jean-Mairet, J., Moudry, R., Amstutz, H., and Bailey, J.E. (1999). Engineered glycoforms of an antineuroblastoma IgG1 with optimized antibody-dependent cellular cytotoxic activity. Nat. Biotechnol. *17*, 176–180.

van de Geijn, F.E., Wuhrer, M., Selman, M.H., Willemsen, S.P., de Man, Y.A., Deelder, A.M., Hazes, J.M., and Dolhain, R.J. (2009). Immunoglobulin G galactosylation and sialylation are associated with pregnancy-induced improvement of rheumatoid arthritis and the postpartum flare: results from a large prospective cohort study. Arthritis Res. Ther. *11*, R193.

Verma, N., Dimitrova, M., Carter, D.M., Crevar, C.J., Ross, T.M., Golding, H., and Khurana, S. (2012). Influenza virus H1N1pdm09 infections in the young and old: evidence of greater antibody diversity and affinity for the hemagglutinin globular head domain (HA1 Domain) in the elderly than in young adults and children. J. Virol. *86*, 5515–5522.

Wang, T.T., Tan, G.S., Hai, R., Pica, N., Petersen, E., Moran, T.M., and Palese, P. (2010). Broadly protective monoclonal antibodies against H3 influenza viruses following sequential immunization with different hemagglutinins. PLoS Pathog. *6*, e1000796.

Washburn, N., Schwab, I., Ortiz, D., Bhatnagar, N., Lansing, J.C., Medeiros, A., Tyler, S., Mekala, D., Cochran, E., Sarvaiya, H., et al. (2015). Controlled tetra-Fc sialylation of IVIg results in a drug candidate with consistent enhanced anti-inflammatory activity. Proc. Natl. Acad. Sci. USA *112*, E1297–E1306.

WHO (2002). WHO Manual on Animal Influenza Diagnosis and Surveillance (World Health Organization).

Wrammert, J., Smith, K., Miller, J., Langley, W.A., Kokko, K., Larsen, C., Zheng, N.Y., Mays, I., Garman, L., Helms, C., et al. (2008). Rapid cloning of high-affinity human monoclonal antibodies against influenza virus. Nature *453*, 667–671.

Wuhrer, M., Stavenhagen, K., Koeleman, C.A., Selman, M.H., Harper, L., Jacobs, B.C., Savage, C.O., Jefferis, R., Deelder, A.M., and Morgan, M. (2015). Skewed Fc glycosylation profiles of anti-proteinase 3 immunoglobulin G1 autoantibodies from granulomatosis with polyangiitis patients show low levels of bisection, galactosylation, and sialylation. J. Proteome Res. *14*, 1657–1665.

Cell

A

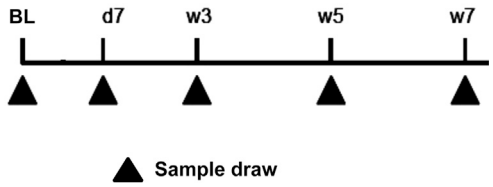

B

Gender (M/F)	5/5
Age (mean years, range)	38.6, 23-50
Race	Caucasian: 4 African American: 4 American Indian: 1 Not disclosed: 1

Figure S1. Study Timeline and Demographic Data, Related to Figures 1, 2, 3, and 4

(A) Sera and PBMCs were drawn prior to vaccination at baseline (BL), day 7, week 3, week 5, and week 7 post-TIV administration. (B) Study demographics.

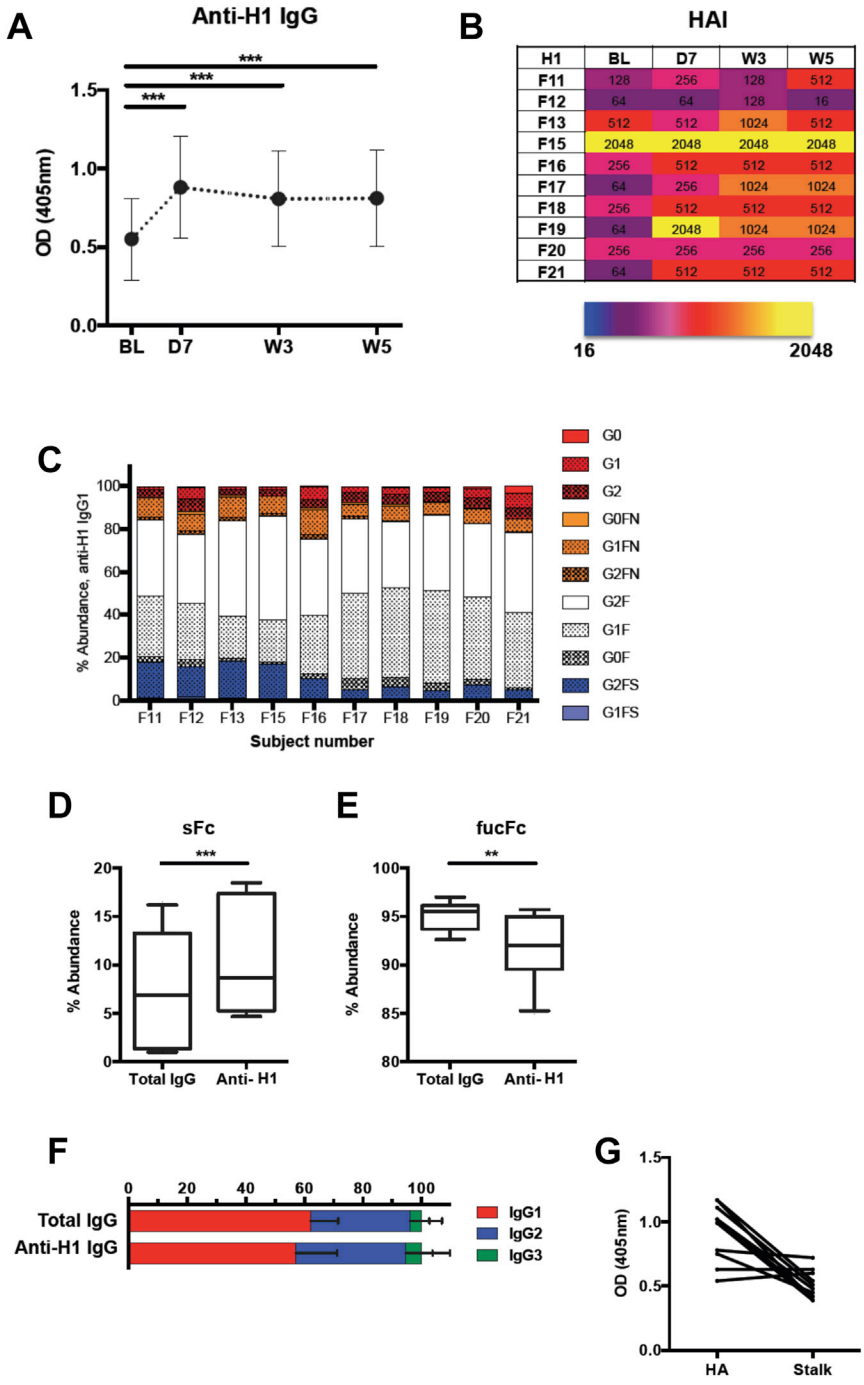

Figure S2. Additional Characterization of TIV Response, Related to Figure 2

Healthy adults were vaccinated with the 2012–2013 seasonal trivalent inactivated influenza virus vaccine. (A) At baseline, all subjects were positive for binding IgG against the H1 hemagglutinin vaccine component from the H1N1 A/California/04/2009 virus (the x axis is not linear) and (B) HAI+ IgG. Titers were elevated by day 7 post-vaccination.(C) Fc glycoforms on baseline anti-H1 IgG. Composition of the core Fc glycan can be modified by addition of fucose (F), N-acetylglucosamine (N), galactose (G) and sialic acid (S). Glycoforms are listed by modifications only – all Fc glycoforms contain the core structure of three mannose residues and four N-acetylglucosamine residues shown in the dotted box in Figure 1D. (D) Anti-H1 IgG1 was significantly more sialylated (sFc) and (E) less fucosylated (fucFc) than total IgG1 from the same donors. (F) Anti-H1 HA IgG1, IgG subclass distribution was not significantly different from the subclass distribution of total IgG. Mean H1-specific IgG1: 56.18% (SD 14.16), IgG2: 37.64% (SD 15.14), IgG3: 5.37% (SD 3.82). Mean total IgG1: 62.17% (SD 9.33), IgG2: 33.94% (SD 10.89), IgG3: 3.88% (SD 2.72). (G) Anti-globular head IgG were in greater abundance in most subjects than anti-stalk IgG at week 3 post-vaccination. $^{**}p < 0.01$; $^{***}p < 0.001$; determined by two-tailed Student's t test.

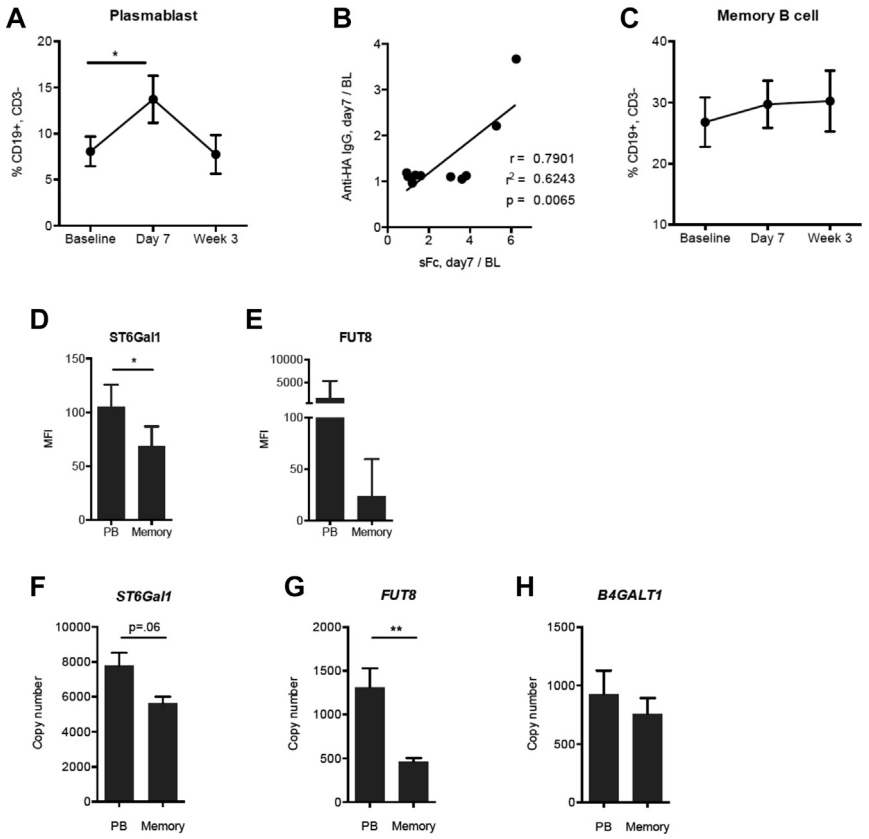

Figure S3. Glycosyltransferase Expression in B Cell Subsets, Related to Figures 2 and 3

(A) PB peaked at day 7 post-vaccination. (B) Fold change in abundance of sFc on total anti-HA IgG correlated with fold change in anti-IgG titer from baseline to day 7 post-vaccination. (C) Memory B cell abundance post-vaccination. (D) B cells from 3 cohort subjects were analyzed for glycosyltransferase expression. ST6Gal1 expression was higher in PB than in memory cells. (E) Elevation in plasmablast FUT8 expression did not reach statistical significance. (F and G) *ST6Gal1* and *FUT8* transcript abundance was greater in total PB than in total memory cells from six patients who received the 2009–2010 TIV. (H) No difference in *B4GALT1* transcript level was observed between PB and memory cells. *$p < 0.05$; **$p < 0.01$; ***$p < 0.001$; ****$p < 0.0001$ determined by two-tailed Student's t test following confirmation of normal distribution. Non-parametric Wilcoxon matched-pairs signed rank test used for (D). Correlation analysis was used to determine the Pearson correlation coefficient, r. Linear regression was used to determine goodness of fit, r^2.

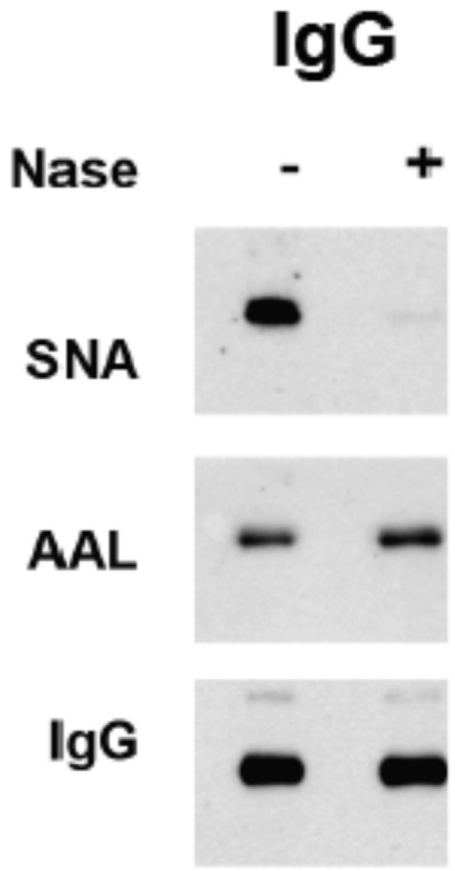

Figure S4. Neuraminidase Treatment of Polyclonal Human IgG Preparations, Related to Figures 5, 6, and 7

Representative western blot demonstrating removal of sialic acids from IgG by neuraminidase treatment. IgGs were probed with *Sambucus nigra* lectin (SNA), which binds preferentially to sialic acid attached to terminal galactose in α-2,6 or α-2,3 linkage, or with *Aleuria aurantia* lectin (AAL), which binds preferentially to fucose linked (α −1,6) to *N*-acetylglucosamine or to fucose linked (α −1,3) to *N*-acetyllactosamine related structures (control lectin), or with anti-Fc (IgG) to detect IgG protein. Neuraminidase treatment removed nearly all sialic acids detectible with SNA lectin from IgG preparations.

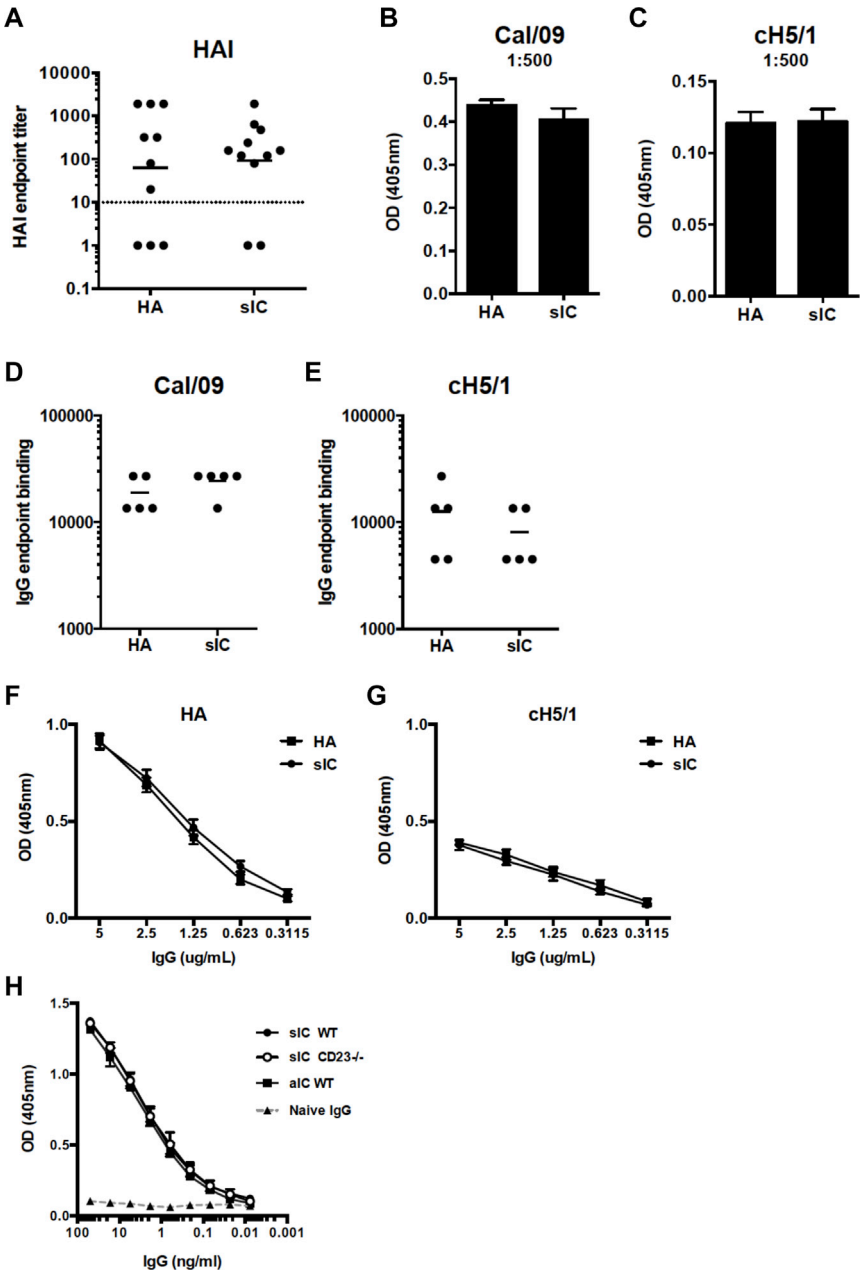

Figure S5. Characterization of IgG Elicited by sIC or HA, Related to Figure 7

(A) HA or sIC priming elicited equivalent HAI titers against virus expressing the homologous HA used in vaccination (Netherlands/602/2009, H1N1). (B and C) Binding titer to Cal/09 protein or to the H1 stalk domain were equivalent in IgG pools elicited by HA or sIC. 1:500 dilution shown was in linear range for both preparations. (D and E) Endpoint binding titer to Cal/09 protein or to the H1 stalk domain in mice immunized with the sIC or HA priming protocol (described in methods). (F and G) Binding curves of purified IgG used in mouse challenge experiments shown in Figures 7A–7D to Cal/09 HA protein or to the cH5/1 H1 stalk domain protein. (H) Binding curves of purified IgG used in mouse challenge experiments shown in Figures 7E–7J to PR8 HA protein; sialylated PY102/PR8 IC (sIC) in wild-type (WT) or CD23-deficient mice (CD23−/−), asialylated PY102/PR8 IC (aIC) in WT or IgG from naive mice (Naive IgG).

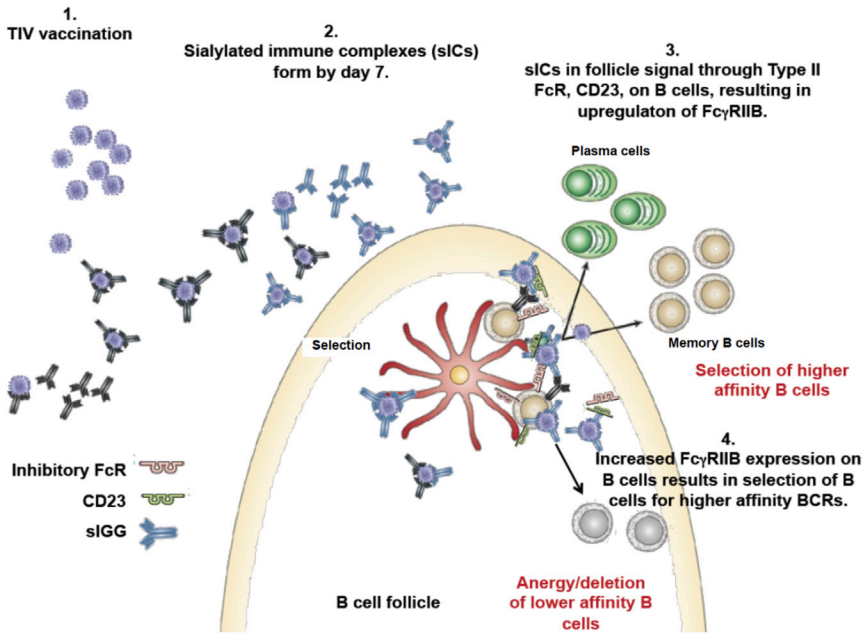

Figure S6. Co-engagement of CD23 and B Cell Receptor Drives Selection of Higher Affinity B Cells, related to Figures 1, 2, 3, 4, 5, 6, and 7

Our studies suggest a model whereby sialylated ICs increase selective pressure on B cells by triggering increased FcγRIIb expression through co-engagment of CD23 and BCR; this results in increased threshold of BCR affinity that is required for cell survival and selection of B cells with higher affinity for antigen, thus elevating the affinity of antibody elicited during vaccination.

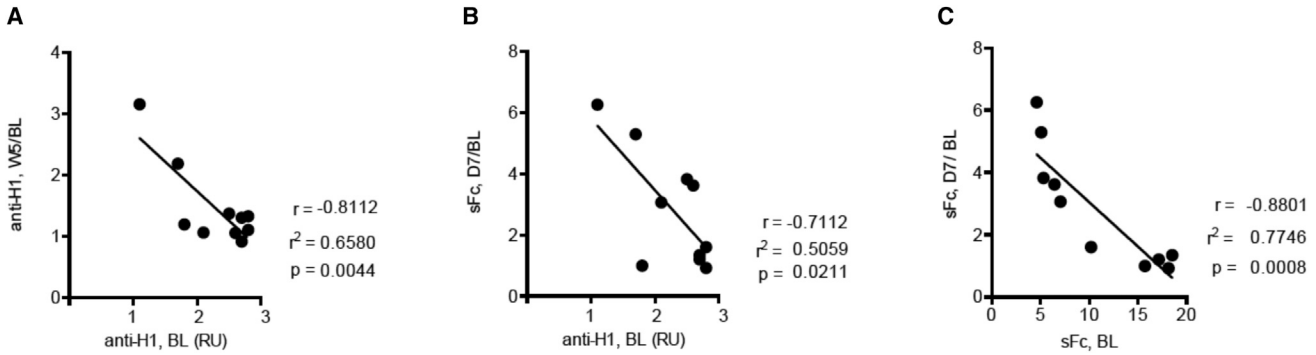

Figure S7. Correlations between Baseline Anti-HA IgG and Subsequent Antibody Response, Related to Figures 1, 2, 3, 4, 5, 6, and 7

(A) The magnitude of anti-H1 IgG present at baseline (anti-H1, BL) correlated negatively with the anti-H1 vaccine response by week 5 (anti-H1, W5/BL) and (B) abundance of sialylated glycoforms produced in the week following vaccination (sFc, D7/BL). (C) Baseline sialylated Fc glycan abundance on anti-H1 IgG (sFc, BL) correlated negatively with the abundance of sialylated glycoforms produced in the week following vaccination. Correlation analysis was used to determine the Pearson correlation coefficient, r. Linear regression was used to determine goodness of fit, r^2.

Cell

Supplemental Information

Anti-HA Glycoforms Drive B Cell Affinity Selection and Determine Influenza Vaccine Efficacy

Taia T. Wang, Jad Maamary, Gene S. Tan, Stylianos Bournazos, Carl W. Davis, Florian Krammer, Sarah J. Schlesinger, Peter Palese, Rafi Ahmed, Jeffrey V. Ravetch

Supplemental Experimental Procedures

Fc Glycan Analysis

Purified IgG or on-bead IgG samples were denatured with 6M guanidine-HCl, reduced with 10 mM DTT at 56 °C for 45 min and alkylated with 60mM iodoacetamide for 1h followed by 30min incubation with 20mM DTT. The samples were trypsin digested (37ºC for 16 h) and desalted using solid phase extraction (SPE) on Sep-Pak Cartridges (Waters, Milford, MA). Tryptic peptides were eluted and evaporated to dryness in a Speedvac SC110 (Thermo Savant) before analysis. Fc glycoforms were specifically identified (Fab glycans excluded) based on tryptic peptide sequence identification. NanoLC-MS/MS analysis for characterization of glycosylation sites was performed on an UltiMate3000 nanoLC (Dionex) coupled with a hybrid triple quadrupole linear ion trap mass spectrometer, the 4000 Q Trap (AB SCIEX).

MS data acquisition was performed using Analyst 1.4.2 software (Applied Biosystems) for precursor ion scan triggered information dependent acquisition (IDA) analysis and enhanced MS-based IDA analysis (Zhang et al., 2012; Zhang and Williamson, 2005). The precursor ion scan of the oxonium ion (HexNAc+ at m/z 204.08) was monitored at a step size of 0.2 Da across a mass range of *m/z* 400 to 1600 for detecting glycopeptides containing N-acetylhexosamine unit. The nanospray voltage was 1.9 kV, and was used in positive ion mode for all experiments. The declustering potential was set at 50 eV and nitrogen as collision gas. In IDA analysis, after each precursor ion scan or EMS scan, and enhanced resolution scan, the two to three highest intensity ions with multiple charge states were selected for tandem MS (MS/MS) with rolling collision energy applied for detected ions based on different charge states and m/z values. All acquired MS/MS spectra from EMS-IDA were subjected to Mascot database search. All acquired MS/MS spectra for detected glycopeptides ions by precursor ion scanning were manually inspected and interpreted with Analyst 1.4.2 and BioAnalysis 1.4 software (Applied Biosystems). The peak areas of detected precursor ions were determined by extracted chromatogram (XIC) at each specific m/z representing glycopeptides isoforms. The relative quantitations of the sugar glycan isoforms of *N*-linked peptide ions were carried out based on precursor ion peak areas under assumption that all sugar glycan isoforms linked to the same core peptide have identical or a similar ionization efficiency. **This method does not discriminate between modifications made to the 1,3 and the 1,6**

arms of the biantennary Fc glycan. The eleven glycoforms analyzed were those present in greatest abundance within our sample set.

Flow Cytometry Analysis

Single-cell suspensions were obtained by forcing spleens of immunized mice through a 70um mesh. Germinal center cells were identified as B220^{+}, FAS^{hi}, CD38^{lo}; light zone cells were additionally CD86^{hi}, CXCR4^{lo}; dark zone cells were additionally CD86lo, CXCR4^{hi}. Antigen-specific peripheral B cells were identified with fluorescent microspheres (Bangs Laboratories Inc.) coupled to Cal/09 HA protein as HA^{+}, CD19^{+}, CD3^{-}. Human PB were identified from PBMCs as CD19^{+}, CD3^{-}, CD20^{lo}, CD38^{hi}, CD27^{hi}, CD138^{-}; human memory cells were identified as CD19^{+}, CD3^{-}, CD20^{+}, CD38^{+}, CD27^{+}, CD138^{-}. Dead cells were excluded by staining with live/dead fixable stain (life technologies). Glycosyltransferase levels were determined using ST6Gal 1-FITC (USBiological) and FUT8-FITC (Bioss), both polyclonal rabbit IgGs (Abcam). A control polyclonal rabbit IgG-FITC antibody was used to determine background binding. Intracellular staining was performed using Cytofix/Cytoperm and Perm/Wash solution as recommended by the manufacturer (BD Biosciences).

Hemagglutination Inhibition Assay

Sera were tested in a standard hemagglutination inhibition assay (WHO, 2002). Briefly, chicken red blood cells and 96-well V-bottom plates (Costar) were used. influenza virus was diluted to 4 hemagglutination units/25µl immediately before use in the HAI assay. Sera were treated with RDE (receptor-destroying enzyme) (Sigma Aldrich) per standard protocol prior to testing. HAI titer was defined as the reciprocal of the greatest dilution that completely inhibited hemagglutination of RBCs. HAI tests were performed twice, in duplicate.

Gene Expression

PBMCs were isolated 7 days post vaccination and PBs and memory cells were isolated by cell sorting. PBs were highly enriched for influenza vaccine-specific cells as demonstrated by ELISPOT. Immediately after sorting, RNA was isolated from approximately 200,000 plasma cells or PB or approximately 1,000,000 CD27+ B cells using the Qiagen RNEasy mini kit. RNA expression levels were determined using Illumina human-6 v2.0 expression beadchips at the Keck Microarray Resource at Yale.

Six replicate RNA samples were analyzed for each cell type. Expression values were normalized for all samples using quantile normalization. Probes IDs for genes shown are: ST6GAL1 ILMN_1756501, FUT8 ILMN_1741422, B4GALT1 ILMN_1766221.

Size Exclusion Chromatography

ICs were generated by incubation of recombinant HA (molar ratio of 1:3 HA:IgG) with either monoclonal anti-HA PY102 or HA-specific IgG isolated from human plasma by affinity purification using recombinant HA. Size of the ICs was determined by size exclusion chromatography using a Superdex 200 10/300 GL column (GE healthcare) on an Akta Pure 25 HPLC system (GE Healthcare). A mix of proteins with varying MW (20-1236 kDa; NativeMark protein standard; Life technologies) was used for size calibration.

Generation and Characterization of Immune Complexes

The polyclonal human ICs were formed by incubation of molar ratio 30:1 polyclonal IgG:HA trimer. Subclass distribution in the IgG preparation was 74.9% IgG1, 20.4% IgG2, 4.5% IgG3, as determined by mass spectrometry. Fc glycoform composition without neuraminidase treatment was 4.2% afucosylated (G0, G1, G2), 17.69% sialylated (G1FS, G2FS), 78.0% neutral (G0F, G1F, G2F, G0FN, G1FN, G2FN). Size of the complexes was determined by HPLC; three peaks corresponding to immune complexes were observed in both the sialylated and asialylated preparations – peak 1: >600 kDa, peak 2: ~537 kDa, peak 3: ~445 kDa. The monoclonal human ICs were generated by incubation of molar ratio 3:1 IgG1:HA trimer. Fc glycoform composition without neuraminidase treatment was 4.5% afucosylated (G0, G1, G2), 23.79% sialylated (G1FS, G2FS), 70.97% neutral (G0F, G1F, G2F, G0FN, G1FN, G2FN). Sialylated glycoforms were not detected following neuraminidase treatment. Size of the complexes was determined by HPLC; one peak corresponding to immune complexes of ~634 kDa was observed in the sialylated and asialylated IC preparation.

References

WHO (2002). WHO Manual on Animal Influenza
Diagnosis and Surveillance, pp. 99.

Zhang, S., Sherwood, R.W., Yang, Y., Fish, T., Chen, W., McCardle, J.A., Jones, R.M., Yusibov, V., May, E.R., Rose, J.K.*, et al.* (2012). Comparative characterization of the

glycosylation profiles of an influenza hemagglutinin produced in plant and insect hosts. Proteomics *12*, 1269-1288.

Zhang, S., and Williamson, B.L. (2005). Characterization of protein glycosylation using chip-based nanoelectrospray with precursor ion scanning quadrupole linear ion trap mass spectrometry. Journal of biomolecular techniques : JBT *16*, 209-219.